



## Research article

## Comparative analysis on the bleaching of crude palm oil using activated groundnut hull, snail shell and rice husk

M.E. Ojewumi<sup>a,\*</sup>, A.B. Ehinmowo<sup>b</sup>, O.R. Obanla<sup>a</sup>, B.M. Durodola<sup>a</sup>, R.C. Ezeocha<sup>a</sup><sup>a</sup> Covenant University, Ota, Ogun state, Nigeria<sup>b</sup> University of Lagos, Akoka, Lagos, Nigeria

## ARTICLE INFO

## Keywords:

Groundnut hull  
Snail shell  
Peroxide value  
Rice husk  
CCD  
Adsorbent  
Bleaching

## ABSTRACT

Researchers have found out several ways by which environmental pollution can be of positive relevance by recycling the waste to ensure a cleaner and healthier environment. The bleaching process is a crucial process in palm oil refining in which an adsorbent is majorly used to adsorb the unwanted colour pigments and a wide range of other impurities. This study aims to modify three different adsorbents; Groundnut hull, Snail shell, and rice husk and processed them into powder form as Groundnut hull powder [GHP], Snail shell powder [SSP] and Rice husk powder [RHP] respectively. The effects of three factors: temperature, mass and time were investigated on the response. MINITAB 19 software was employed which resulted in 20 runs. The optimization of the bleaching effects imposed by the adsorbents on palm oil using Central Composite Design (CCD) was evaluated. The free fatty acid and peroxide value decrease with bleaching while the saponification value increased with bleaching. The analysis conducted shows that groundnut hull was able to adsorb the most significant value of FFA and peroxide value in the palm oil. The lowest value of FFA obtained indicates that bleaching increases the shelf life of the oil and makes it more suitable for soap making.

## 1. Introduction

Pollution has become a massive problem for the environment in many countries including Nigeria. Various waste materials are usually discarded indiscriminately leading to environmental pollution by littering and burning [1]. The accumulation of excessive volumes of solid waste such as papers, industrial and kitchen waste and the search for clean energy are topical global issues [2]. Recycling of waste by some industries has greatly helped in curbing environmental pollution, as these materials are now recycled re-used instead of wasting them. Several research has been carried out on various ways by which pollutants can be of positive relevance to guarantee a healthier environment such as bioconversion of waste paper to glucose, waste citrus and sweet potato peel to biodiesel [3, 4, 5, 6].

Food processing companies generates waste during the process of a converting raw materials to useful products [7, 8]. Researchers have worked on the conversion of biodegradable portion of food waste such as orange peel to produce essential product [9]. The increasing amount of food waste and other materials will become a big problem to the environment if there is no reasonable solution such as the conversion into biodiesel or other useful materials [10, 11].

There has been an increase in the dumping of used bleaching materials despite the laws and regulations [12, 13, 14]. Most of the bleaching materials used in Nigeria are traditional and some of them cannot be recycled, hence contributing to environmental pollution [15, 16, 17]. This can be curbed to an extent through the use of renewable agricultural waste products in bleaching processes [18, 19].

Palm oil is one of the critical oil crops in various West African countries; it contains characteristic food substances and inorganic segments, whereupon life and adventures depend [20]. Oil palm is used in various food products, such as margarine, shortenings, cooking oils, and confectionery fats. Assessment has revealed that it can, in like manner use as a fuel mixture for inward consuming engines. It is accordingly essential for creators in West Africa to fabricate creation and to improve the planning method to extend oil yield [20].

According to reports, natural clay, carbon activated clay, and acid-activated clay can also bleach crude palm oil [21, 22]. However, the use of clay in bleaching crude palm oil has been postulated to be very costly, non-environmental friendly, non-renewable, and ineffective, significantly the carbon activated clay [23, 24].

Design of experiment through Mathematical model is a decision making tool that assists in effectively making decisions which involves

\* Corresponding author.

E-mail address: [modupe.ojewumi@covenantuniversity.edu.ng](mailto:modupe.ojewumi@covenantuniversity.edu.ng) (M.E. Ojewumi).

some complex issues [25, 26, 27, 28]. This compares the effects of input factors (input variables) on response (output variable) simultaneously. It is basically used to determine cause-and-effect relationships, which is required to process inputs in order to optimize the experimental outputs. Factors are changed in order to observe the changes it has on the response variables. Experimental design is an effective process in planning experiments so that the data obtained can be analysed to yield viable and objective conclusions [28, 29, 30].

This study aims to modify these three different adsorbents; groundnut hull, snail shell, and rice husk, and evaluate their bleaching efficiency on palm oil.

## 2. Materials and methods

See Figures 1, 2, and 3.



Figure 1. Groundnut Hull.



Figure 2. Snail shell.



Figure 3. Rice husk.

### 2.1. Experimental procedures

The distinctive examination was done on the adsorbents GHP, SHP, RHP and palm oil. The moisture content and debris content were done using the AOCs Recommended Practice Ca 2f-93 technique, and the peroxide value was done using the methodology proposed.

### 2.2. Processing of adsorbent

Samples were carefully screened for foreign bodies. Snail shell and Groundnut hull were washed carefully with deionized water to remove particulate material from their surface. Samples were later dried in oven at 100 °C for 24 h before pulverizing to powder form and sieved with the aid of a mechanical sieve to standardize particle size.

### 2.3. Physico-chemical analysis of adsorption

**2.3.1. Moisture content.** One gram of the dried adsorbents was measured and put in a dry crucible. The crucible was set in a spray dryer at 105 °C for 2 h.

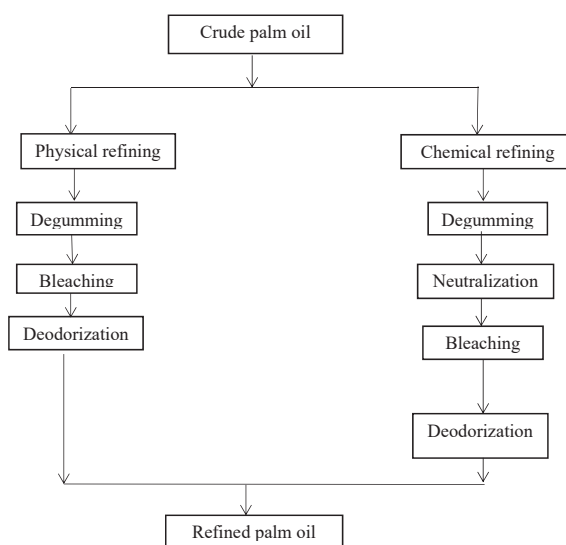


Figure 4. Methods of crude palm oil refining.

**Table 1.** Physico-chemical properties of the unrefined palm oil before adsorption.

Analysis	Result
FFA (mg KOH/g)	7.43
Peroxide value (mEq./kg)	12.5
Moisture content	0.4
Saponification value (mg KOH/g)	195
Density (kg/m <sup>3</sup> )	921
Acid value (mg KOH/g)	14.9
Specific gravity	0.9
Ester value	173
Molecular weight (g/mol)	968

**Calculations:**

$$\text{Moisture \%} = \frac{\text{loss in weight on drying}}{\text{initial weight}} \times 100 \tag{1}$$

**2.3.2. Ash content.** One gram of the buildup adsorbent sample was moved into a crucible and sample was then positioned in a furnace, the temperature was allowed to rise to 1000 °C for 1 h 30 min. After which it was cooled in a desiccator.

**Calculations:**

$$\text{Ash content} = \frac{Wc\&s - Wc}{W_o} \tag{2}$$

Wc&s = weight of the crucible and sample after ash testing  
 Wc = Weight of the adsorbent before ash testing

**2.4. Physico-chemical analysis of palm oil**

**2.4.1. Moisture content.** As indicated by [32], the crucibles were washed and oven dry. They were later cooled in the desiccator and weigh. 2 g The sample was placed in it [33, 34]. Samples were dried in the spray dryer at 80 °C for 2 h and at 135 °C for 4 h and afterward cooled in the desiccator, after which the dry load of the sample in addition to crucible was taken.

**Table 2.** Randomized Central Composite Design of the experiment using MINI-TAB 19.

Run order	Mass (g) [X1]	Temperature (°C) [X2]	Time (mins) [X3]
1	1.8	100	60
2	0.8	110	90
3	3.5	100	60
4	2.8	110	90
5	1.8	100	60
6	0.8	110	30
7	1.8	100	110
8	0.8	90	30
9	0.8	90	90
10	1.8	100	60
11	1.8	100	60
12	2.8	110	30
13	1.8	117	60
14	2.8	90	30
15	1.8	83	60
16	0.1	100	60
17	1.8	100	60
18	2.8	90	90
19	1.8	100	9
20	1.8	100	60

**Table 3.** Proximate analysis on the bleached palm oil using groundnut hull as adsorbent (GHP).

Mass (g)	Temperature (°C)	Time (mins)	FFA (mg KOH/g)	POV (mEq/kg)
1.8	100	60	3.72	4.431
0.8	110	90	5.281	12.452
3.5	100	60	0.781	0.872
2.8	110	90	0.932	0.951
1.8	100	60	3.72	4.431
0.8	110	30	6.302	12.632
1.8	100	110	2.152	2.532
0.8	90	30	6.421	6.753
0.8	90	90	6.215	6.423
1.8	100	60	3.72	4.431
1.8	100	60	3.72	4.431
2.8	110	30	0.954	12.513
1.8	117	60	1.326	12.733
2.8	90	30	0.981	1.240
1.8	83	60	6.942	8.231
0.71	100	60	7.121	7.321
1.8	100	60	3.72	4.431
2.8	90	90	1.036	1.072
1.8	100	9	7.092	8.924
1.8	100	60	3.72	4.431

**Calculation:**

$$\% \text{ Moisture} = \frac{W_2 - W_3}{W_2 - W_1} \times 100 \tag{3}$$

Where:

W<sub>1</sub> = Initial weight of the empty crucible  
 W<sub>2</sub> = Weight of crucible plus sample before drying  
 W<sub>3</sub> = Final weight of crucible plus food after drying

**2.4.2. Peroxide value.** The technique detailed by [31] in their work was utilized. 1 g of oil sample was measured and poured in a dry 250 ml conical flask. 10 ml of chloroform was included, and the oil thoroughly

**Table 4.** Proximate analysis on the bleached palm oil using rice husk as adsorbent.

Mass (g)	Temperature (°C)	Time (mins)	FFA (mg KOH/g)	POV (mEq/kg)
1.8	100	60	4.705	9.542
0.8	110	90	6.402	12.763
3.5	100	60	0.923	9.340
2.8	110	90	0.912	12.543
1.8	100	60	4.705	9.542
0.8	110	30	6.972	12.634
1.8	100	110	3.532	6.042
0.8	90	30	7.033	7.211
0.8	90	90	6.730	6.903
1.8	100	60	4.705	9.542
1.8	100	60	4.705	9.542
2.8	110	30	0.976	12.512
1.8	117	60	1.613	12.931
2.8	90	30	1.243	2.531
1.8	83	60	7.163	9.764
0.71	100	60	7.321	9.752
1.8	100	60	4.705	9.542
2.8	90	90	1.072	1.843
1.8	100	9	7.301	10.475
1.8	100	60	4.705	9.542

**Table 5.** Proximate analysis on the bleached palm oil using Snail shell as adsorbent.

Mass (g)	Temperature (°C)	Time (mins)	FFA (mg KOH/g)	POV (mEq/kg)
1.8	100	60	5.042	10.041
0.8	110	90	6.740	13.432
3.5	100	60	0.532	9.634
2.8	110	90	0.837	12.837
1.8	100	60	5.042	10.041
0.8	110	30	6.943	13.213
1.8	100	110	4.872	8.241
0.8	90	30	7.023	9.042
0.8	90	90	6.924	8.82
1.8	100	60	5.042	10.041
1.8	100	60	5.042	10.041
2.8	110	30	1.043	12.673
1.8	117	60	4.973	13.631
2.8	90	30	1.320	4.370
1.8	83	60	5.410	8.403
0.71	100	60	7.084	8.638
1.8	100	60	5.042	10.041
2.8	90	90	0.956	7.63
1.8	100	9	7.352	6.07
1.8	100	60	5.042	10.041

mixed together. 15 ml of acid and 1 ml of potassium iodide were included. The flask with stopper was shaken for one minute and put in a dark locker for one minute, 75 ml of water was included, and the blended sample was titrated with 0.002 M sodium thiosulphate solvent starch (1%) as a pointer. The titre value was recorded as (V), and the precise worth (VO) was recorded.

**Calculations:**

$$\text{Peroxide value (mEq/kg)} = \frac{(V - VO)}{M} \times 10^3 \tag{4}$$

Where: T = exact molarity of sodium thiosulphate solution.

**2.4.3. Acid value and free fatty acid content.** The technique by [32] and [35] was utilized. 10 ml of n - propanol was blended with 10 ml of diethyl ether and, 1 ml of Phenolphthalein (1%) was included. 2 g of oil was disintegrated in the Solvent and titrated with 0.1 M KOH, shaking continually until a pink shading which endured for 15 sec was obtained. The measure of KOH utilized was recorded.

**Calculation:**

$$\text{Acid value (mg KOH/g)} = \frac{\text{Titre value} \times 5.61}{\text{Sample weight}} \tag{5}$$

$$\text{Free fatty acid (mg KOH/g)} = \frac{\text{Acid value}}{2} \tag{6}$$

**2.4.4. Ester value.** The ester value was acquired by [31] by finding the contrast between the saponification value and acid value.

**2.4.5. Saponification value.** 2 g of oil were measured precisely and placed in a conical flask containing 25 ml of 0.5 M alcoholic KOH. The reflux condenser was fitted to the jar containing the ionic solution and warmed in a water shower for an hour, whirling the flask habitually. Abundance KOH was titrated with 0.5 M HCl with 1 ml of phenolphthalein (1%) solution. The technique was repeated for the blank.

$$\text{Saponification value (mg KOH/g)} = \frac{(b - a) \times 28.05}{\text{sample weight}} \tag{7}$$

**2.5. Chemical/physical mechanism involved in the bleaching process**

The mechanism involved in the bleaching process is shown in Figure 4.

**3. Results**

See Tables 1 and 2.

**3.1. Regression equation in uncoded units**

The uncoded regression equation is shown in equation 8. See Tables 3, 4, 5, 6, and 7; Figures 5, 6, 7, and 8.

**Table 6.** Plan application for the cycle simulation on the % FFA yield of groundnut hull (GHP).

Std. order	Run order	Pt-Type	Blocks	Mass (g)	Temperature (°C)	Time (mins)	%FFA [Response]		
							Experimental	Predicted	Residual
17	1	0	1	1.8	100	60	3.72	3.77	0.05
7	2	1	1	0.8	110	90	5.281	4.25	-1.03
10	3	-1	1	3.5	100	60	0.781	0.93	0.15
8	4	1	1	2.8	110	90	0.932	0.26	-0.67
19	5	0	1	1.8	100	60	3.72	3.77	0.05
3	6	1	1	0.8	110	30	6.302	6.18	-0.12
14	7	-1	1	1.8	100	110	2.152	3.06	0.90
1	8	1	1	0.8	90	30	6.421	7.74	1.32
5	9	1	1	0.8	90	90	6.215	6.26	0.04
18	10	0	1	1.8	100	60	3.72	3.77	0.05
16	11	0	1	1.8	100	60	3.72	3.77	0.05
4	12	1	1	2.8	110	30	0.954	1.55	0.60
12	13	-1	1	1.8	117	60	1.326	2.49	1.12
2	14	1	1	2.8	90	30	0.981	2.65	1.67
11	15	-1	1	1.8	83	60	6.942	5.05	-1.89
9	16	-1	1	0.1	100	60	7.121	7.40	0.28
15	17	0	1	1.8	100	60	3.72	3.77	0.05
6	18	1	1	2.8	90	90	1.036	1.80	0.77
13	19	-1	1	1.8	100	9	7.092	5.37	-1.73
20	20	0	1	1.8	100	60	3.72	3.77	0.05
Total							75.856	77.587	1.731

**Table 7.** Investigation of change (ANOVA) for the reaction surface regression.

Source	DF	Adj SS	Adj MS	F-Value	P-Value
Model	9	86.06	9.56	5.71	0.006
Linear	3	85.15	28.38	16.96	0.000
Mass [X1]	1	70.27	70.27	41.99	0.000
Temp [X2]	1	8.27	8.27	4.94	0.050
Time [X3]	1	6.61	6.61	3.95	0.075
Square	3	0.50	0.17	0.10	0.958
Mass*Mass [X1*X1]	1	0.09	0.09	0.05	0.826
Temp*Temp [X2*X2]	1	0.00	0.00	0.00	0.972
Time*Time [X3*X3]	1	0.37	0.37	0.22	0.648
2-Way Interaction	3	0.40	0.13	0.08	0.969
Mass*Temp [X1X2]	1	0.11		0.1063	0.060
Mass*Time [X1X3]	1	0.11	0.19	0.12	0.738
Temp*Time [X2X3]	1	0.09	0.09	0.06	0.812
Error	10	16.74	1.67		
Lack-of-Fit	5	16.73	3.34	*	*
Pure Error	5			0.000	0.0000
Total	19			102.794	

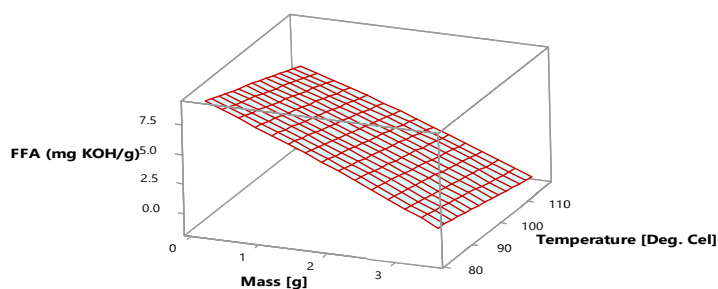


**Figure 5.** 3D surface plot of FFA for groundnut hull vs. mass and temperature.

$$\begin{aligned} \%FFA = & 16.6 - 3.46 (\text{Mass}) - 0.052 (\text{Temp}) - 0.017 (\text{Time}) - 0.077 \\ & (\text{Mass} \times \text{Mass} \ 0.00012) (\text{Temp} \times \text{Temp}) + 0.000178 (\text{Time} \times \text{Time}) + 0.0115 \\ & (\text{Mass} \times \text{Temp}) + 0.0053 (\text{Mass} \times \text{Time}) - 0.00037 (\text{Temp} \times \text{Time}) \end{aligned} \quad (8)$$

**3.1.1. Regression equation**

See Table 8; Figures 10, 11, and 12.

$$\text{Peroxide value} = -7.91 - 2.710 \times \text{mass} + 0.2229 \times \text{temperature} - 0.0561 \times \text{time} \quad (9)$$

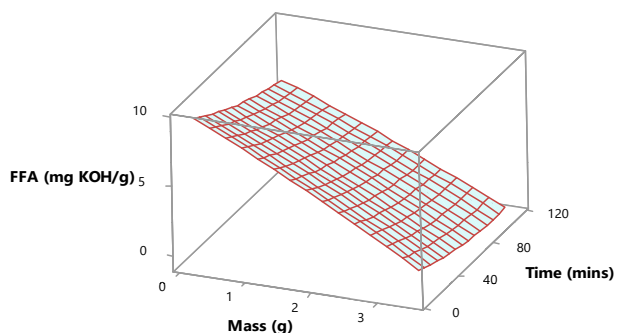


**Figure 6.** 3D surface plot of FFA for groundnut hull vs. mass and time.

**3.1.2. Regression equation**

See Table 9; Figures 13, 14, 15, and 16.

$$\% \text{ FFA} = 17.76 - 0.01825 \times \text{time} - 0.0744 \times \text{temperature} - 2.654 \times \text{mass} \quad (10)$$

**3.1.3. Regression equation**

See Table 10; Figures 17, 18, 19, and 20.

$$\text{Peroxide value} = -15.08 - 0.867 \times \text{mass} + 0.2710 \times \text{temperature} - 0.0202 \times \text{time} \quad (11)$$

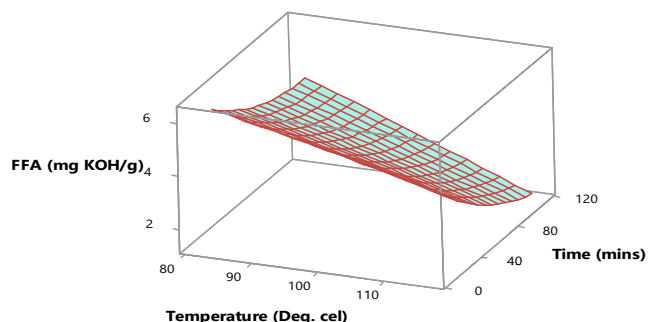


**Figure 7.** 3D surface plot of FFA for groundnut hull vs. temperature and time.



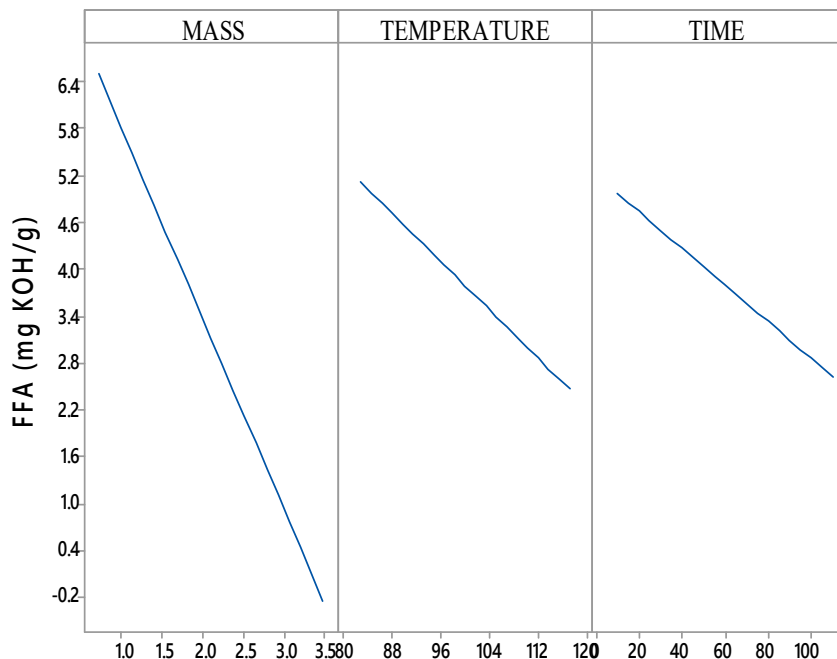


Figure 8. Factorial plot of FFA for groundnut hull vs. time, temperature and mass.

3.1.4. Regression equation

See Table 11; Figures 21, 22, 23, and 24.

$$\%FFA = 11.40 - 2.745 \times \text{mass} - 0.0102 \times \text{temperature} - 0.1242 \times \text{time} \quad (12)$$

$$\text{Peroxide value} = -12.91 - 0.501 \times \text{mass} + 0.2710 \times \text{temperature} - 0.0202 \times \text{time} \quad (13)$$

3.1.5. Regression equation

See Table 12; Figures 25, 26, 27, and 28.

3.2. Physicochemical properties of the palm oil after adsorption

See Tables 13, 14, 15.

Table 8. Plan application for the cycle simulation on the POV yield of groundnut hull (GHP).

Std. order	Run order	Pt-Type	Blocks	Mass (g)	Temperature (°C)	Time (mins)	Peroxide value [Response]		
							Experimental	Predicted	Residual
17	1	0	1	1.8	100	60	4.431	6.1416	1.7106
7	2	1	1	0.8	110	90	12.452	9.3983	-3.0537
10	3	-1	1	3.5	100	60	0.872	1.5351	0.6631
8	4	1	1	2.8	110	90	0.951	3.9790	3.028
19	5	0	1	1.8	100	60	4.431	6.1416	1.7106
3	6	1	1	0.8	110	30	12.632	12.7619	0.1299
14	7	-1	1	1.8	100	110	2.532	3.3386	0.8066
1	8	1	1	0.8	90	30	6.753	8.3042	1.5512
5	9	1	1	0.8	90	90	6.423	4.9407	-1.4823
18	10	0	1	1.8	100	60	4.431	6.1416	1.7106
16	11	0	1	1.8	100	60	4.431	6.1416	1.7106
4	12	1	1	2.8	110	30	12.513	7.3425	-5.1705
12	13	-1	1	1.8	117	60	12.733	9.9306	-2.8024
2	14	1	1	2.8	90	30	1.240	2.8848	1.6448
11	15	-1	1	1.8	83	60	8.231	2.3526	-5.8784
9	16	-1	1	0.17	100	60	7.321	9.0952	1.7742
15	17	0	1	1.8	100	60	4.431	6.1416	1.7106
6	18	1	1	2.8	90	90	1.072	-0.4787	-1.5507
13	19	-1	1	1.8	100	9	8.924	9.0006	0.0766
20	20	0	1	1.8	100	60	4.431	6.1416	1.7106
Total							121.325	121.325	4.441 × 10 <sup>-15</sup>

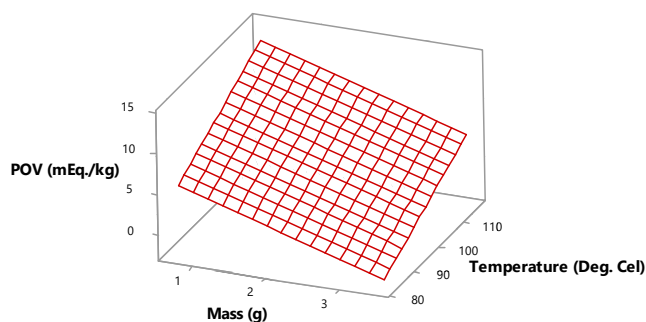


Figure 9. 3D surface plot of POV for groundnut hull vs. mass and temperature.

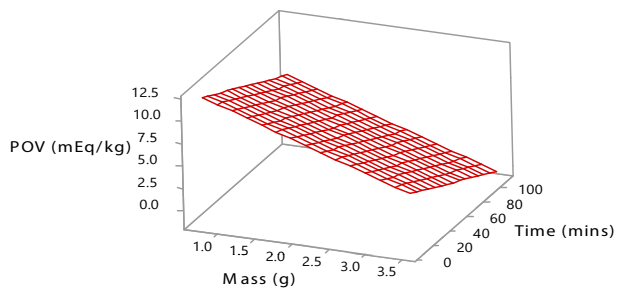


Figure 10. 3D surface plot of POV for groundnut hull vs. mass and time.

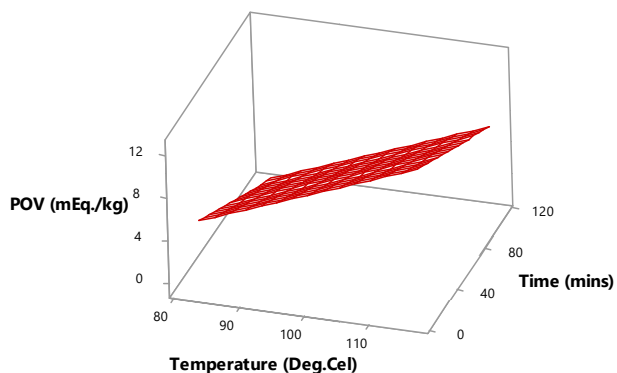


Figure 11. 3D surface plot of POV for groundnut hull vs. temperature and time.

## 4. Discussion of result

### 4.1. Activation of adsorbents

The three adsorbents used in this work; snail shell, rice husk, and groundnut hull, were subjected to an activation reaction using a strong acid ( $H_2SO_4$ ) so as to effectively bleach the palm oil. Previous work done has shown a high reduction in the impurities present in palm oil as a result of contact with bleaching adsorbents, such as used in this work. From the research work carried out by [36] on activation of Oyster shell, the time of activation was modified in this present work for the activation (using  $H_2SO_4$ ) on the adsorbent samples for 5 h to analyze the influence of time on the surface area increment.

### 4.2. Analysis of groundnut hull on the response (FFA)

Table 1 shows the physico-chemical properties of palm oil before bleaching. The estimation of the free unsaturated fat (7.43%) shows that palm oil is still new and fresh; therefore a decrease in FFA is required. The free unsaturated fat is among the undesirable constituents to be eliminated, and its low rate will, in general, improve the effectiveness of the

refining cycle [37]. The moisture content, which has a low value, shows why the free unsaturated fat is impressively low.

Ref. [31] also reported that the moisture content influences the free unsaturated fat rate in the oil. Saponification estimation of 195 mgKOH/kg recommends that the palm oil can be utilized for soap production. Table 2 shows a randomized central composite design [CCD] of the investigation, which acquired utilizing the MINITAB 19 software. These information arrangements were taken to the laboratory and used to acquire the test estimations of the reaction towards the palm oil's bleaching.

From Tables 3, 4, and 5, the information of the free fatty acid (FFA) and peroxide value (POV) impact by the adsorbents were illustrated. The information was acquired utilizing the randomized design of the experimental result obtained from MINITAB 19 and contained 20 runs that were examined independently. For each run, the bleaching cycle was done using the set components which incorporate; mass, temperature, and time to show its impact on the cycle.

From Table 6, the optimum FFA percentage is 0.781%, with an optimum condition of 3 g of activated GHP at 100 °C and 60 min. Other FFA values include 0.932, 0.954, 0.981, and 1.036, with 2.8 g of activated GHP as the most occurring quantity, the temperature within the range of 110 and 90 °C, and duration of 90 and 30 min, respectively. It also indicated the predicated values obtained using the regression equation in the MINITAB software, set to a confidence level of 95%. It provides future researchers with a range of values they can use to carry out similar research. From the table, researchers can be 95% certain that the range of values would be between 0.26% to 7.74%.

Table 7 shows the investigation of change (ANOVA) for the centrality of the model insights. The model's centrality was carried out using Fisher dissemination (F-value and P-value) with huge F-value and a little P-value model to anticipate the reactions successfully, and this recommends a high degree of the regression model. The model's nature is anticipated by the F-value while observing all the elements used to plan the model simultaneously. The likelihood of acquiring little or immaterial results on the reaction can be described as the P-value. Preferable model fitness to the data obtained experimentally was signified by larger F-values. In addition, for a statistically important model, the P-value should be below 0.05. To determine the fitness of the model equation,  $R^2$  (determination coefficient) was used to determine the regression model. This measures the level of variability in the values of the experimental response, which can be analyzed by the variables and their relations.

The response surface plots for groundnut hull were obtained with the MINITAB 19 programming. They show the connection between the response and the indicator factors, which are the elements (mass, temperature, and time) used to screen the fading effectiveness. The product draws out the impact of just two elements on the response, while the other is kept constant.

#### 4.2.1. Effect of GHP dosage on the FFA response

Figure 5 shows the relationship between the response and the factors considered in this research. The factor of mass and temperature were used to monitor the response while time is held constant by the software. From the figure, it is evident that there is a decrease in the FFA present in the oil as mass increases. Figure 6 also shows the relationship between the response and the factors. In this scenario, the factors of mass and time are used to monitor the response while temperature is kept constant. It is visible from the selected figure that there is a significant reduction in the response as the mass increases. The response also decreases with time, but it is not as immediate as that of mass.

#### 4.2.2. Effect of temperature on the FFA response

Figure 5, as stated earlier, shows the complicated relationship between the response and the factors. Here, the element of mass and temperature are varied while time is held constant. The plot shows that as the temperature of the process increased, the response decreased. The surface plot, represented by Figure 7, shows the relationship between the response and the factors. Unlike the previous

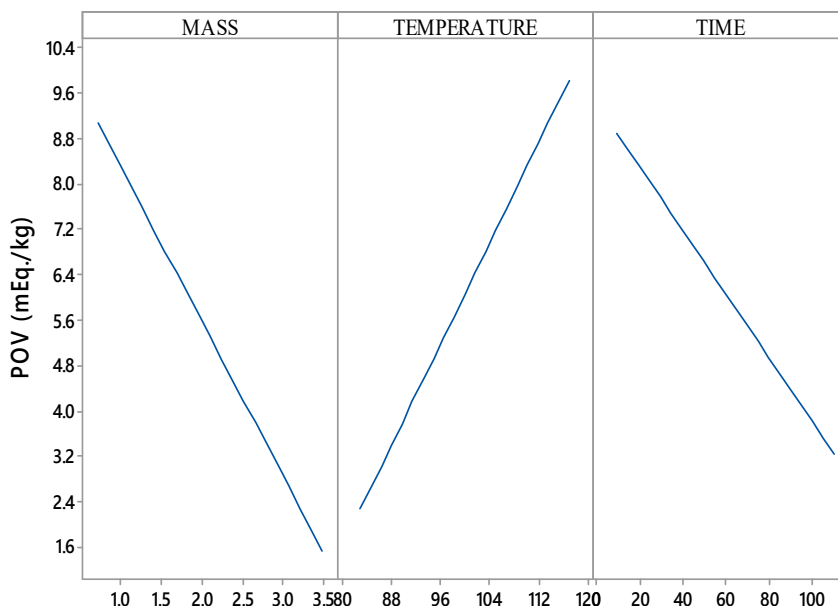


Figure 12. Factorial plot of POV for groundnut hull vs. mass, temperature and time.

Table 9. Plan application for the cycle simulation on the % FFA yield of rice husk (RHP).

Std. order	Run order	Pt-Type	Blocks	Mass (g)	Temperature (°C)	Time (mins)	%FFA [Response]		
							Experimental	Predicted	Residual
17	1	0	1	1.8	100	60	4.705	4.45120	-0.2538
7	2	1	1	0.8	110	90	6.402	5.81407	-0.58793
10	3	-1	1	3.5	100	60	0.923	-0.06127	-0.98427
8	4	1	1	2.8	110	90	0.912	0.50529	-0.40671
19	5	0	1	1.8	100	60	4.705	4.45120	-0.2538
3	6	1	1	0.8	110	30	6.972	6.90930	-0.0627
14	7	-1	1	1.8	100	110	3.532	3.53851	0.00651
1	8	1	1	0.8	90	30	7.033	8.39711	1.36411
5	9	1	1	0.8	90	90	6.730	7.30188	0.57188
18	10	0	1	1.8	100	60	4.705	4.45120	-0.2538
16	11	0	1	1.8	100	60	4.705	4.45120	-0.2538
4	12	1	1	2.8	110	30	0.976	1.60051	0.62451
12	13	-1	1	1.8	117	60	1.613	3.18656	1.57356
2	14	1	1	2.8	90	30	1.243	3.08832	1.84532
11	15	-1	1	1.8	83	60	7.163	5.71583	-1.44717
9	16	-1	1	0.17	100	60	7.321	7.34448	0.02348
15	17	0	1	1.8	100	60	4.705	4.45120	-0.2538
6	18	1	1	2.8	90	90	1.072	1.99309	0.92109
13	19	-1	1	1.8	100	9	7.301	5.38214	-1.91886
20	20	0	1	1.8	100	60	4.705	4.45120	-0.2538
Total							87.1885	87.42334	0.23484

models, the factor of mass is kept constant while temperature and time are used to monitor the response. The increase in temperature affected the response, which led to its reduction. But compared to the previous figures that displayed the mass factor, we can denote that the adsorbent mass has a more significant effect on the response data. Bleaching temperatures usually range from 90 °C–125 °C, according to [38]. He also noted that oil viscosity decreases with heightened temperature resulting in better particle dispersion and enhanced interactions with clay oil. Refs. [38] and [39] stated that the optimum bleaching temperature is specific for a particular adsorbent and oil between 100 °C and 120 °C for palm oil, making the optimum temperature approved for this process assumed range.

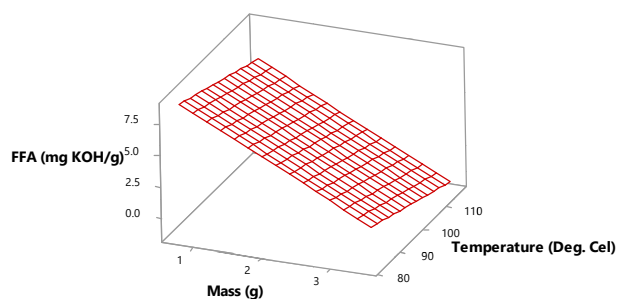


Figure 13. 3D surface plot of FFA for rice husk vs. mass and temperature.



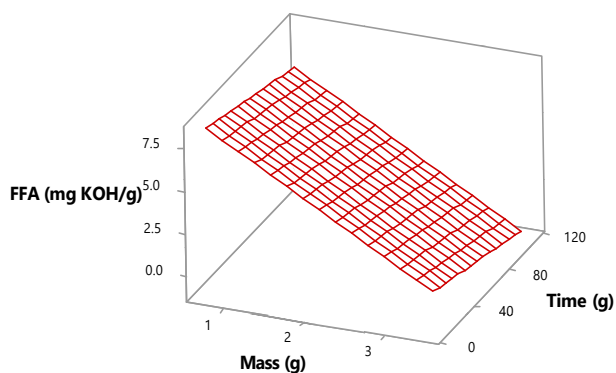


Figure 14. 3D surface plot of FFA for rice husk vs. mass and time.

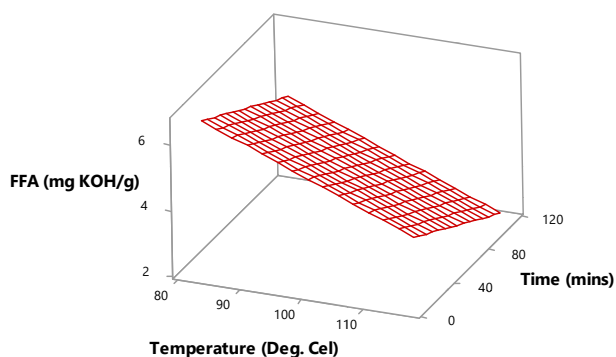


Figure 15. 3D surface plot of FFA for rice husk vs. temperature and time.

4.2.3. Effect of time on the FFA response

The longer it takes for a process to be actualized, the longer the process reactions. Figure 6 shows an exact representation of the time effect on the response. Previously stated, the temperature factor is kept constant while there is a relationship between the response and the factors of mass and time. From the plot, as the adsorption time

increases, there is a reduction in the response. The plot shown in Figure 7 represents the relationship between the response and the factors; temperature and time. It is observed that as the time of adsorption increases, there is a deduction in the free fatty acid (response). This is expected because, as stated earlier, the longer the processing time, the longer the process reaction. It follows the work of [36], who stated that the bleaching efficiency increase with the processing time.

Figure 8 is a simplified factorial plot that summarizes the surface plots. From this figure, we can denote that an increase in the mass, temperature, and time of the adsorption process decreases the free fatty acid present in the palm oil, with mass having the highest effect.

4.3. Analysis on the POV (response) for GHP

Table 8 shows the design of the experiment in Table 2. These experimental data were obtained in the laboratory and the predicted values given by the MINITAB 19 software using the regression equation in Eq. (2). The optimal mass of this analysis was 0.71 g at a temperature of 117 °C and 9 min. As stated earlier, the predicted value was obtained using a regression equation and a set confidence level of 95%. From the predicted data, researchers can be confident that when working on a similar project, the range of values to be obtained would be between -0.4787% and 12.7619%.

4.3.1. Effect of GHP dosage on the POV response

Figure 9 is a surface response plot that shows the effect of the adsorbent mass on the response. The plot consists of the continuous variables, mass, and temperature, while time is kept constant, and their effect on the response is investigated. As the adsorbent mass increases, there is a reduction in the response. Figure 10 also shows the relationship between the response and the continuous variables. In this scenario, the factor of mass and time is monitored while the temperature is kept constant. The surface plot shows a deduction in the peroxide value present as the mass increased.

4.3.2. Effect of temperature on the POV response

According to [40], peroxide value is susceptible to heat and excess temperature. Table 8 shows that the POV increased at a very high

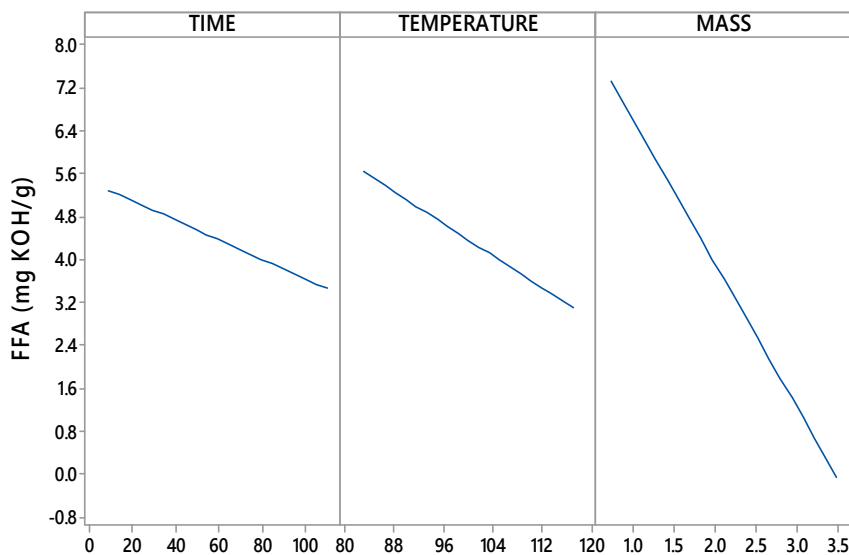


Figure 16. Factorial plot of FFA for rice husk vs. time, temperature and mass.

**Table 10.** Plan application for the cycle simulation on the POV yield of rice husk (RHP).

Std. order	Run order	Pt-Type	Blocks	Mass (g)	Temperature (°C)	Time (mins)	Peroxide value [Response]		
							Experimental	Predicted	Residual
17	1	0	1	1.8	100	60	9.542	9.2502	-0.2918
7	2	1	1	0.8	110	90	12.763	12.2232	-0.5398
10	3	-1	1	3.5	100	60	9.340	7.7757	-1.5643
8	4	1	1	2.8	110	90	12.543	10.4884	-2.0546
19	5	0	1	1.8	100	60	9.542	9.2502	-0.2918
3	6	1	1	0.8	110	30	12.634	13.4326	0.7986
14	7	-1	1	1.8	100	110	6.042	8.2424	2.2004
1	8	1	1	0.8	90	30	7.211	8.0121	0.8011
5	9	1	1	0.8	90	90	6.903	6.8026	-0.1004
18	10	0	1	1.8	100	60	9.542	9.2502	-0.2918
16	11	0	1	1.8	100	60	9.542	9.2502	-0.2918
4	12	1	1	2.8	110	30	12.512	11.6979	-0.8141
12	13	-1	1	1.8	117	60	12.931	13.8578	0.9268
2	14	1	1	2.8	90	30	2.531	6.2773	3.7463
11	15	-1	1	1.8	83	60	9.764	4.6427	-5.1213
9	16	-1	1	0.17	100	60	9.752	10.1957	0.4437
15	17	0	1	1.8	100	60	9.542	9.2502	-0.2918
6	18	1	1	2.8	90	90	1.843	5.0678	3.2248
13	19	-1	1	1.8	100	9	10.475	10.2783	-0.1967
20	20	0	1	1.8	100	60	9.542	9.2502	-0.2918
Total							184.496	184.4957	-0.0003

temperature. Figure 9 visualizes the table by showing the effect of the factors on the response. Time is held constant while mass and temperature are the variables. As the temperature increased to 110 °C, there was an increase in the peroxide value, and other causes could be overheating when the experiment was carried out. Likewise, Figure 11 shows a similar result as that of Figure 9. Here, the continuous variables are temperature and time, while the mass is kept constant, and the trend of the POV was on the decline as the process temperature increased.

4.3.3. Effect of time on the POV response

An increase in the time of a process increases the reaction. From the data outlined in Table 8 to the plot represented by Figures 9 and 11, the increase in process time reduced the peroxide value, and it might have resulted from the rise in the time at which the adsorbent spent in the oil. Figure 11 illustrates a factorial plot that summarizes the response surface plots. It makes interpretation easy for readers and from the figure which consist of two negative and one positive slope, we can denote that as the mass and time increases, the POV reduces but as the temperature increased to the maximum, the POV increased (see Figure 12).

4.4. Analysis of rice husk on the response (FFA)

Groundnut hull adsorbent and its effect on the response (FFA and POV) was discussed and it was noted that amongst the three factors, mass

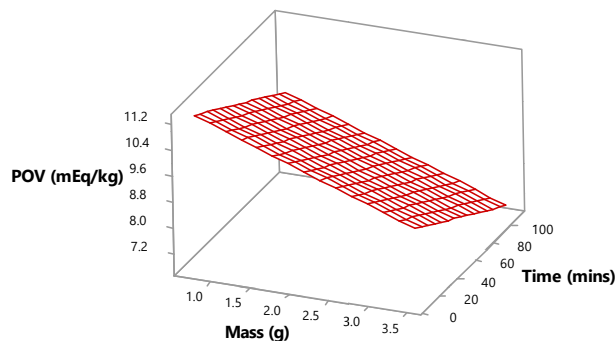


Figure 18. 3D surface plot of POV for rice husk vs. mass and time.

has the highest effect on the response reduction. Table 9 comprises of the experimental result which showcases the FFA data obtained in the laboratory, predicted column which contains data calculated using a regression equation. The optimal mass of this analysis was 0.71 g at a temperature of 83 °C and 9 min. A confidence level of 95% was set because it is the most common and the default level of the software. It was set to give the researchers a cue on what to expect when undergoing

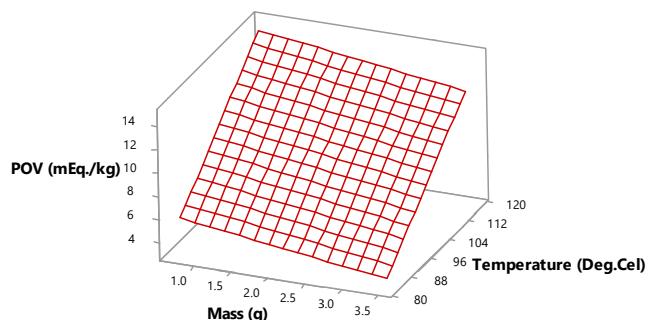


Figure 17. 3D surface plot of POV for rice husk vs. mass and temperature.

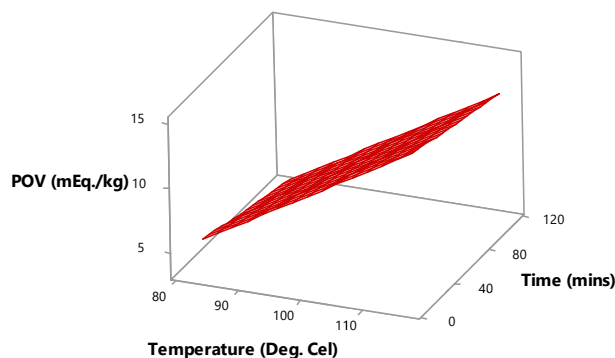


Figure 19. 3D surface plot of POV for rice husk vs. temperature and time.

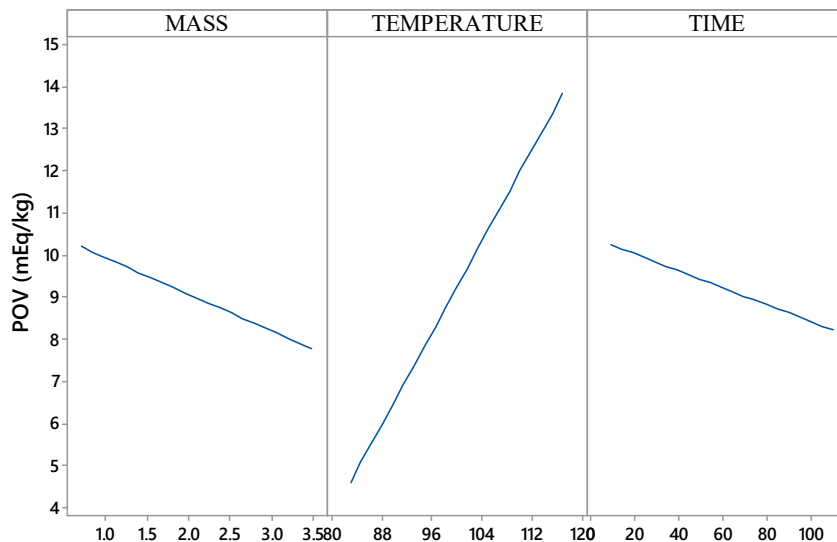


Figure 20. Factorial plot of POV for rice husk vs. time, temperature and mass.

Table 11. Plan application for the cycle simulation on the % FFA yield of snail shell (SSP).

Std. order	Run order	Pt-Type	Blocks	Mass (g)	Temperature (°C)	Time (mins)	%FFA [Response]		
							Experimental	Predicted	Residual
17	1	0	1	1.8	100	60	5.042	4.69615	-0.34585
7	2	1	1	0.8	110	90	6.740	6.96678	0.22678
10	3	-1	1	3.5	100	60	0.532	0.02945	-0.50255
8	4	1	1	2.8	110	90	0.837	1.47654	0.63954
19	5	0	1	1.8	100	60	5.042	4.69615	-0.34585
3	6	1	1	0.8	110	30	6.943	7.71216	0.76916
14	7	-1	1	1.8	100	110	4.872	4.07500	-0.797
1	8	1	1	0.8	90	30	7.023	7.91577	0.89277
5	9	1	1	0.8	90	90	6.924	7.17039	0.24639
18	10	0	1	1.8	100	60	5.042	4.69615	-0.34585
16	11	0	1	1.8	100	60	5.042	4.69615	-0.34585
4	12	1	1	2.8	110	30	1.043	2.22192	1.17892
12	13	-1	1	1.8	117	60	4.973	4.52308	-0.44992
2	14	1	1	2.8	90	30	1.320	2.42553	1.10553
11	15	-1	1	1.8	83	60	5.410	4.86923	-0.54077
9	16	-1	1	0.17	100	60	7.084	7.68833	0.60433
15	17	0	1	1.8	100	60	5.042	4.69615	-0.34585
6	18	1	1	2.8	90	90	0.956	1.68015	0.72415
13	19	-1	1	1.8	100	9	7.352	5.32973	-2.02227
20	20	0	1	1.8	100	60	5.042	4.69615	-0.34585
Total							92.261	92.26096	-4E-05

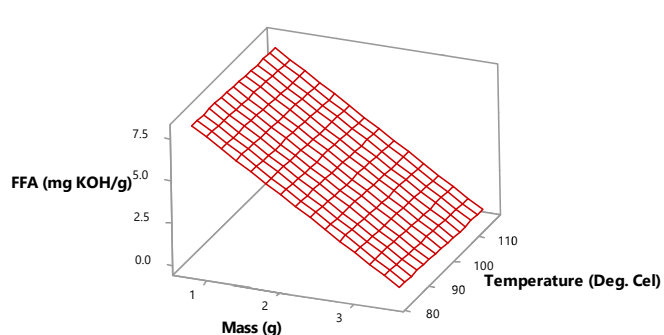


Figure 21. 3D surface plot of FFA for snail shell vs. mass and temperature.

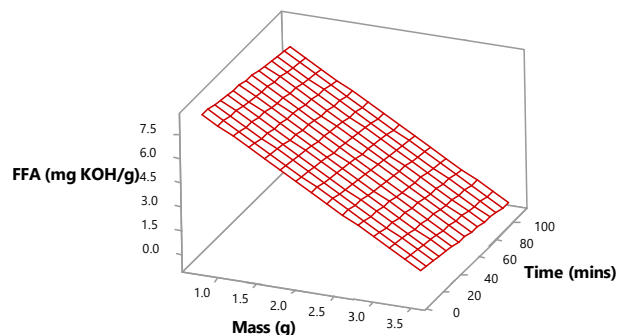


Figure 22. 3D surface plot of FFA for snail shell vs. mass and time.

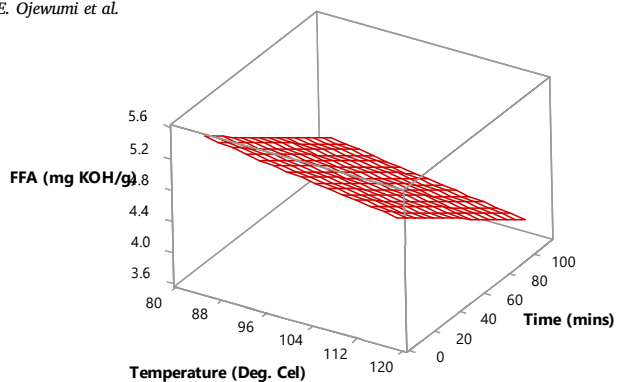


Figure 23. 3D surface plot of FFA for snail shell vs. temperature and time.

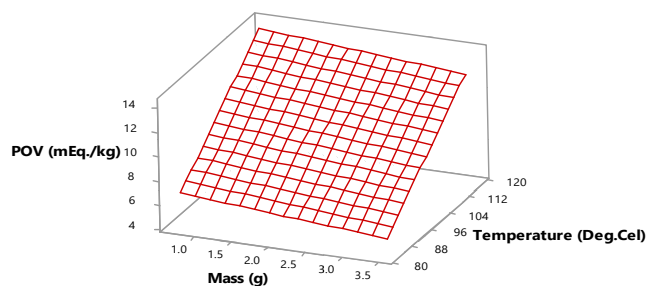


Figure 25. 3D surface plot of POV for snail shell vs. mass and temperature.

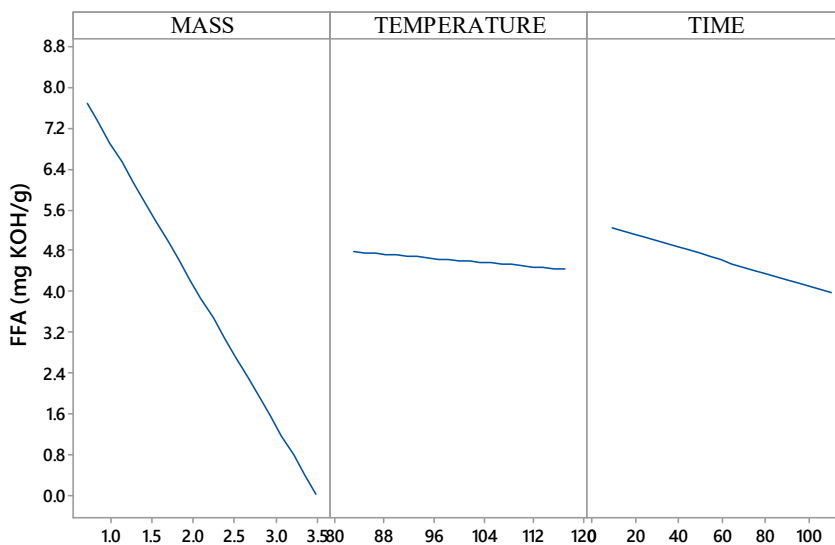


Figure 24. Factorial plot of FFA for snail shell vs. time, temperature and mass.

Table 12. Plan application for the cycle simulation on the POV of snail shell (SSP).

Std. order	Run order	Pt-Type	Blocks	Mass (g)	Temperature (°C)	Time (mins)	Peroxide value [Response]		
							Experimental	Predicted	Residual
17	1	0	1	1.8	100	60	10.041	9.8601	-0.1809
7	2	1	1	0.8	110	90	13.432	13.1480	-0.284
10	3	-1	1	3.5	100	60	9.634	9.0087	-0.6253
8	4	1	1	2.8	110	90	12.837	12.1463	-0.6907
19	5	0	1	1.8	100	60	10.041	9.8601	-0.1809
3	6	1	1	0.8	110	30	13.213	12.0995	-1.1135
14	7	-1	1	1.8	100	110	8.241	10.7339	2.4929
1	8	1	1	0.8	90	30	9.042	7.5740	-1.468
5	9	1	1	0.8	90	90	8.820	8.6225	-0.1975
18	10	0	1	1.8	100	60	10.041	9.8601	-0.1809
16	11	0	1	1.8	100	60	10.041	9.8601	-0.1809
4	12	1	1	2.8	110	30	12.673	11.0978	-1.5752
12	13	-1	1	1.8	117	60	13.631	13.7068	0.0758
2	14	1	1	2.8	90	30	4.370	6.5723	2.2023
11	15	-1	1	1.8	83	60	8.403	6.0135	-2.3895
9	16	-1	1	0.17	100	60	8.638	10.4061	1.7681
15	17	0	1	1.8	100	60	10.041	9.8601	-0.1809
6	18	1	1	2.8	90	90	7.630	7.6208	-0.0092
13	19	-1	1	1.8	100	9	6.070	8.9689	2.8989
20	20	0	1	1.8	100	60	10.041	9.8601	-0.1809
Total							196.88	196.8797	-0.0003

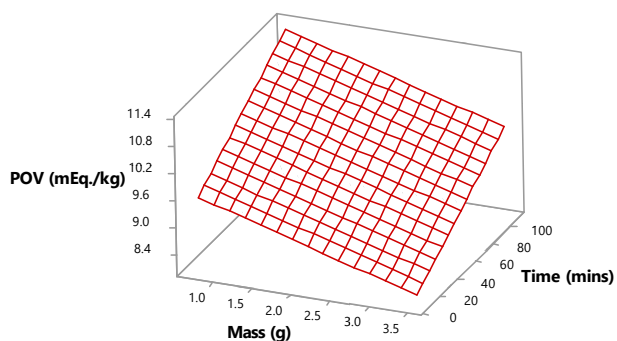


Figure 26. 3D surface plot of POV for snail shell vs. mass and time.

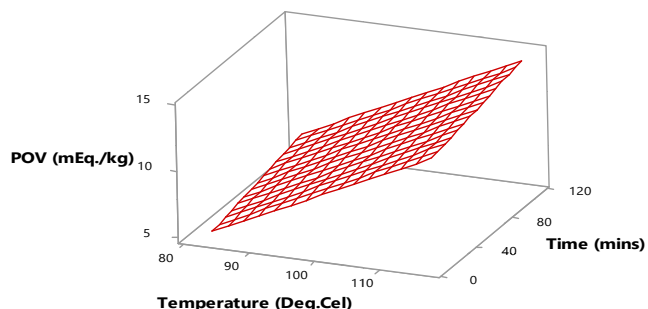


Figure 27. 3D surface plot of POV for snail shell vs. temperature and time.

a similar project. It is noted that the range of values might be between -0.06127% and 7.30188%.

4.4.1. Effect of RHP dosage on the FFA response

Figure 13 represents the surface plot for the FFA response. It contains the relationship between the response variable and two predictor variables (mass and temperature) while time is kept constant. This plot

Table 13. 1.8 g of bleached palm oil at 100 °C for 60 min.

Analysis	GHP	RHP	SHP
FFA (mg KOH/g)	3.720	4.705	5.042
Peroxide value (mEq./kg)	4.431	9.542	10.041
Acid value (mg KOH/g)	7.44	9.41	10.084
Saponification value (mg KOH/g)	201	197	230

visualizes the effect of the mass on the FFA, and it can be noted that as the mass of the rice husk increased, the FFA reduced, which could result from an increase in the active sites for adsorption. The plot represented by Figure 14 also shows the effect of mass on the response. Here, two predictor variables are mass and time, while the temperature is held constant. As the mass of the adsorbent increased, there was a reduction in the FFA response.

4.4.2. Effect of temperature on the FFA response

The surface plot in Figure 13 shows the effect of temperature on the response. As the temperature of the adsorbent increased, the FFA also increased. Figure 15 also portrays the effect of temperature; from the plot, it can be noted that the reduction of FFA is directly proportional to the increase in temperature. It can be pointed out that the temperature effect on the adsorbent has a way of reducing the response but it is not as effective as that of the groundnut hull adsorbent.

4.4.3. Effect of time on the FFA response

Amongst the surface plots created for the rice husk adsorbent on the response, Figure 14 and Figure 15 shows the effect of time. There are two predictor variables and one response variable here. In Figure 14, the predictor variables are mass and time, showing the effect of time. As time increases, there is a reduction in the FFA. This is understandable due to the increase in the period the adsorbent spends in the adsorbate. The surface plot in Figure 15 showcases similar results as that of Figure 14, but in this case, the predictor variables are temperature and time.

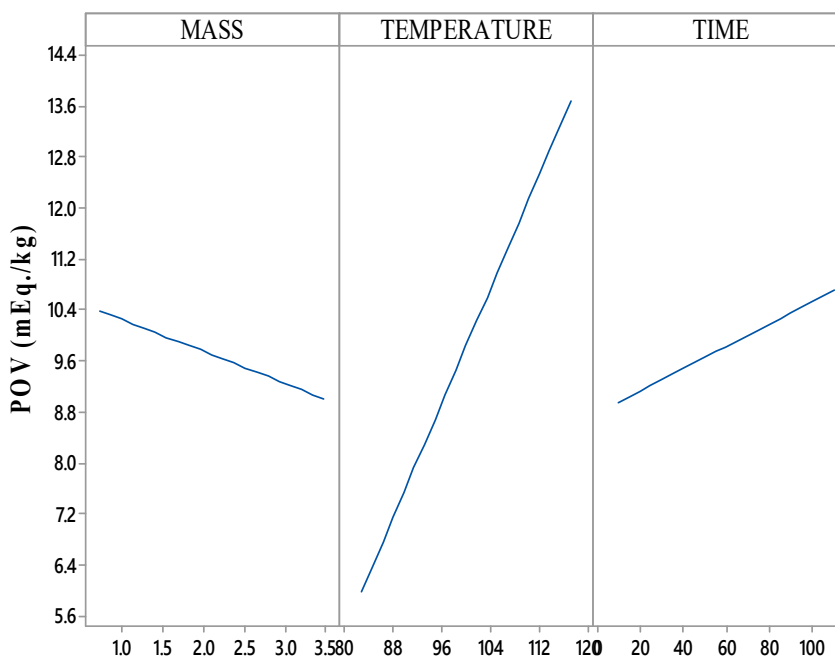


Figure 28. 3D surface plot of POV for snail shell vs. time, temperature and mass.



**Table 14.** 2.8 g of bleached palm oil at 110 °C for 90 min.

Analysis	GHP	RHP	SHP
FFA (mg KOH/g)	0.932	0.912	0.837
Peroxide value (mEq./kg)	0.951	12.543	12.837
Acid value (mg KOH/g)	1.864	1.824	1.674
Saponification value (mg KOH/g)	224	215	247

**Table 15.** 3.5 g of bleached palm oil at 100 °C for 60 min.

Analysis	GHP	RHP	SHP
FFA (mg KOH/g)	0.781	0.923	0.532
Peroxide value (mEq./kg)	0.872	9.340	9.634
Acid value (mg KOH/g)	1.562	1.846	1.064
Saponification value (mg KOH/g)	237	260	272

Figure 16 is a simplified factorial plot that summarizes the surface plots above. They are all negative downward slopes that show an increase in the mass, temperature, and time of the adsorption process decreases the free fatty acid present in the palm oil, with mass having the highest effect.

#### 4.5. Analysis on the POV (response) for RHP

Table 10 shows the design of the experiment in Table 2. These experimental data were obtained in the laboratory and the predicted values given by the MINITAB 19 software using the regression equation in Eq. (3). The optimal mass of this analysis was 0.71 g at a temperature of 83 °C and 9 min. As stated earlier, the predicted value was obtained using a regression equation and a set confidence level of 95%. From the predicted data, there is a certainty scientists can move to the lab by realizing that the scope of qualities would be somewhere in the range of 5.0678% and 13.8578%.

##### 4.5.1. Effect of RHP dosage on the POV response

According to [41], FFA content is the most common property for determining palm oil quality, as it must not exceed 5% alongside the peroxide value. The surface response plots in Figures 17 and 18 shows the 3D effect of the predictor variables on the response variables. Figure 17 shows the relationship between the response and the predictor variables (mass and temperature) while time is held constant. From the plot, it is evident that the increase in the adsorbent mass decreases the POV in the palm oil. The same result is witnessed in Figure 18, where the effect of the predictor variables (mass and time) on the response is monitored. This shows that the adsorbent can reduce peroxide value, but its effect is lesser when compared to the plot of groundnut hull.

##### 4.5.2. Effect of temperature on the POV response

Peroxide value is susceptible to heat and excess temperature, so it is expected to obtain a similar trend as that of groundnut hull. Figures 17 and 19 shows the 3D effect of the variables on the response. From the plot of Figure 17, the predictor variables are mass and temperature. The effect of temperature is observed, and it is deduced that an increase in temperature increases the POV when rice husk is used. Figure 19 also shows a similar result, but the comparison is made with time while the temperature is held constant by the software.

##### 4.5.3. Effect of time on the POV response

From the data outlined in Table 10 to the plot represented by Figures 18 and 19, the increase in process time reduced the peroxide value, and it might have resulted from the rise in the period at which the adsorbent spent in the oil. Figure 18 shows the relationship between the response variable and two predictor variables (mass and time), while the variable of temperature and time is shown in Figure 19. Figure 20 illustrates a factorial plot that summarizes the response surface plots. From

the figure, which consists of two negative and one positive slope, we can denote that as the mass and time increase, the POV reduces but as the temperature increases to the maximum, the POV increases. When compared to the groundnut hull plot, it is observed that the hull has a more reducing effect on the POV to mass and time compared to rice husk.

#### 4.6. Analysis of snail shell on the response (FFA)

Table 11 shows the plan application for the cycle simulation on the % FFA yield of snail shell powder. It contains the design of the experiment shown in Table 2, experimental FFA values that were obtained from the laboratory and predicted values that was obtained from the software (MINITAB 19) using a regression equation represented by Eq. (12). A confidence level of 95% was set because it is the most common and the default level of the software. It was set to give the researchers a cue on what to expect when undergoing a similar project. It is noted that the range of values might be between 0.02945% and 7.91577%.

##### 4.6.1. Effect of SHP dosage on the FFA response

Figures 21 and 22 show the 3D effect of the predictor variable (mass) on the response while time and temperature are held constant respectively. Similar to the previous adsorbents, the surface plots show that as the mass of the SHP increases, the response reduces and this can be attributed to the increasing active sites available for adsorption.

##### 4.6.2. Effect of temperature on the FFA response

Figure 23 conceives the 3D effect of temperature on the response. It comprises the relationship between the response variable (FFA) and the two predictor variables (mass and temperature) while time is held constant. It is evident that the increase in the temperature at which the process was subjected to increase the FFA rate declined. The surface plot represented by Figure 24 also shows a similar trend, but in this scenario, the predictor variables are mass and time while the temperature is held constant.

##### 4.6.3. Effect of time on the FFA response

The time variable is another factor taken into consideration in this segment. The longer the process's time, the more the process reaction occurs, and Figure 21 portrays this statement. The software's surface response plot shows that as the reaction time increases, the FFA decreases. Likewise, Figure 23 shows the 3D effect of the predictor variables (temperature and time) on the response. There is a decrease in the FFA as the time of adsorption increases. The difference between the figures mentioned above is their surface representation.

#### 4.7. Analysis of snail shell on the response (POV)

Table 12 shows the experimental data, predicted values, and the design of the experiment. The experimental values were obtained from the laboratory using the experiment's design as a basis/guide. The predicted data were obtained from the MINITAB 19 software by setting the confidence level to 95% and using a regression model as indicated by Eq. (13).

##### 4.7.1. Effect of SHP dosage on the POV response

According to [41], FFA content is the most common property for determining palm oil quality, as it must not exceed 5% alongside the peroxide value. The surface response plots in Figures 25 and 26 shows the 3D effect of the predictor variables on the response variables. Figure 25 shows the relationship between the response and the predictor variables (mass and temperature) while time is held constant. From the plot, it is evident that the increase in the adsorbent mass decreases the POV in the palm oil. The same result is witnessed in Figure 26, where the effect of the predictor variables (mass and time) on the response is monitored. When comparing the factorial plots of the snail shell to that of groundnut hull, it is visible that their increase in mass, which might have been due to the rise in the active sites, led to the reduction of peroxide value. Still,

groundnut hull shows more effect on the response reduction than the others.

#### 4.7.2. Effect of temperature on the POV response

Figures 25 and 27 shows the 3D effect of the variables on the response. From the plot of Figure 27, the predictor variables are mass and temperature. The effect of temperature is observed, and it is deduced that an increase in temperature increases the POV when snail shell is used. Figure 27 also shows a similar result, but the comparison is made with time while the temperature is held constant by the software.

#### 4.7.3. Effect of time on the POV response

An increase in the time of a process increases the process reaction. From the data outlined in Table 12 to the plot represented by Figures 26 and 27, the increase in process time reduced the peroxide value, and it might have resulted from the rise in the period at which the adsorbent spent in the oil. Figure 26 shows the relationship between the response variable and two predictor variables (mass and time), while the variable of temperature and time is shown in Figure 27. Figure 28 illustrates a factorial plot that summarizes the response surface plots. From the model, which consists of two negative and one positive slope, we can denote that as the mass and time increase, the POV reduces but as the temperature increases to the maximum, the POV increases. Compared to the groundnut hull plot and rice husk, it is observed that they all reduce the POV at high temperatures, but the groundnut hull has the highest effect.

#### 4.8. Physicochemical properties of the palm oil after adsorption

Tables 13, 14, and 15 show the palm oil's Physico-chemical properties after adsorption and it varied at different masses. From these tables, it is evident that the adsorbent has some effect on palm oil. Table 1 shows a vast difference between the palm oil properties before and after adsorption. The free fatty acid (FFA) was reduced upon an adsorbent addition, and this is expected. According to [42], free fatty acid in cooking oil lies within the limits of 0%–3%. Although this range was not achieved by the 1.8 g mass, the FFA values obtained for the others, 2.8 g and 3.5 g, show proximity to the set range. Hence, we can attribute the reduction of FFA to mass. The low value of free fatty acid indicates that palm oil is fresh and will be prolonged.

The peroxide value test is used to determine the oxidative rancidity of the oil. The lower the peroxide value, the longer it stays without deterioration. Likewise, oil with high peroxide value quickly becomes rancid. The peroxide value decreased drastically with the increase in mass and time of the groundnut hull analysis from this report. However, there was a significant increase in the POV as the process temperature increased to certain levels. This is also evident in rice husk analysis, but the reduction of the POV is not as significant as that of GHP [43]. The snail shell analysis also shows a similar result, but the response decreases as the mass increases but is directly proportional to the increase in time and temperature. The increase in temperature can be related to the work of [36], who stated that the peroxide value of palm oil is highly sensitive to heat and high temperature.

The saponification value increased with adsorption, and it indicates that palm oil can be used for soap making.

## 5. Conclusion

The three adsorbents have the ability to bleach crude palm oil effectively. There is no need for the disposal of these wastes materials since they can be processed into something valuable for the palm oil industries. The saponification value increases with bleaching, and the highest values were obtained for the snail shell bleached palm oil. The increase in the saponification value indicates that the oil is very suitable for soap making. The FFA decreased with bleaching; amongst the three adsorbent, the lowest FFA value was obtained for groundnut hull

bleached palm oil followed by snail shell and rice husk. The reduction in FFA prolongs the oil shelf life. The Adsorption process made the palm oil lighter, and this was observed for all adsorbents, but the palm oil bleached with groundnut hull appeared more transparent, indicating it adsorbed more impurities. The oil's peroxide value decreased for mass and time for the groundnut hull and rice husk and increased for temperature. This is as a result of the sensitivity of oil peroxide value to high temperature and heat. In conclusion, the groundnut hull has the lowest FFA and peroxide value from the obtained data, making it the best option for bleaching, although the other adsorbents are effective. Optimum condition of 0.781% FFA was obtained at 3 g of absorbent at 100 °C and 60 min. Since good property of bleaching was recorded at the range of 3 g–2.8 g, it can be concluded that either amount/quantity should be used as absorbent holding other variables constant. Determination of FFA in bleached palm oil was successfully optimized using CCD with three variables. The predictive ability of the model was close to accurate using MINITAB 19 software with the design application for the process simulation for % FFA yield to have 75.856% for experimental and 77.587% for predicted yield with just 1.731% residual.

## Declarations

### Author contribution statement

M.E. Ojewumi: Conceived and designed the experiments; Wrote the paper.

A.B. Ehinmowo: Analyzed and interpreted the data.

O.R. Obanla & B.M. Durodola: Contributed reagents, materials, analysis tools or data.

R.C. Ezeocha: Performed the experiments.

### Funding statement

This work was supported by Covenant University, Ota, Nigeria.

### Data availability statement

Data will be made available on request.

### Declaration of interests statement

The authors declare no conflict of interest.

### Additional information

No additional information is available for this paper.

## References

- [1] M.E. Ojewumi, et al., Alkaline pre-treatment and enzymatic hydrolysis of waste papers to fermentable sugar, *J. Environ. Eng. Ecol. Sci.* 19 (1) (2018) 211–217.
- [2] K. Mokatse, H. Mhlanga, J. van Wyk, Relative saccharification and initial degradation rates of different waste paper materials by cellulase from *Trichoderma viride*, *J. Appl. Biosci.* 105 (1) (2016) 10183–10190.
- [3] R.A. Kerr, Global warming is changing the world, *Science* 316 (5822) (2007) 188–190.
- [4] Ojewumi, M.E., et al., Anaerobic Decomposition of Cattle Manure Blended with Food Waste for Biogas Production.
- [5] M.E. Ojewumi, et al., Pozzolan properties of waste agricultural biomass-African locust bean pod waste, *World J. Environ. Biosci.* 6 (3) (2014) 1–7.
- [6] M.E. Ojewumi, et al., Bioconversion of waste foolscap and newspaper to fermentable sugar, *J. Ecol. Eng.* 20 (4) (2019) 35–41.
- [7] F. Raganati, et al., Butanol production from leftover beverages and sport drinks, *BioEnergy Res.* 8 (1) (2015) 369–379.
- [8] M.E. Ojewumi, et al., Investigation into alternative energy sources from waste citrus peel (orange): approach to environmental protection, *J. Phys.: Conference Series* 1378 (2019), 022066. IOP Publishing.
- [9] M.E. Ojewumi, et al., Bio-conversion of sweet potato peel waste to BioEthanol using *Saccharomyces cerevisiae*, *Bio-Conversion of Sweet Potato Peel Waste to BioEthanol Using Saccharomyces Cerevisiae* 8 (3) (2018) 46–54.

- [10] M.E. Ojewumi, et al., Co-digestion of cow dung with organic kitchen waste to produce biogas using *Pseudomonas aeruginosa*, IOP Conf. Series: J. Phys.: Conf. Series 1299 (2019), 012011.
- [11] M.E. Ojewumi, et al., Bioconversion of orange peel waste by *Escherichia coli* and *Saccharomyces cerevisiae* to ethanol, Int. J. Pharmaceut. Sci. Res. 10 (3) (2018) 1246–1252.
- [12] O.I. Nkwachukwu, N.I. Chidi, K.O. Charles, Issues of roadside disposal habit of municipal solid waste, environmental impacts and implementation of sound management practices in developing country “Nigeria”, Int. J. Environ. Sci. Dev. 1 (5) (2010) 409–418.
- [13] K. Marsh, B. Bugusu, Food packaging—roles, materials, and environmental issues, J. Food Sci. 72 (3) (2007) R39–R55.
- [14] S.K. Loh, K.Y. Cheong, J. Salimon, Surface-active physicochemical characteristics of spent bleaching earth on soil-plant interaction and water-nutrient uptake: a review, Appl. Clay Sci. 140 (2017) 59–65.
- [15] G. Hole, A.S. Hole, Improving recycling of textiles based on lessons from policies for other recyclable materials: A minireview, Sustain. Prod. Consumpt. (2020).
- [16] O.B. Ezeudu, et al., Sustainable production and consumption of paper and paper products in Nigeria: a review, Resources 8 (1) (2019) 53.
- [17] C.S. Ezeonu, et al., Biotechnological tools for environmental sustainability: prospects and challenges for environments in Nigeria—a standard review, Biotechnol. Res. Int. 2012 (2012).
- [18] P.S. Varbanov, X. Jia, J.S. Lim, Process assessment, integration and optimisation: the path towards cleaner production, J. Cleaner Product. 281 (2021) 124602.
- [19] N.K. Arora, et al., Environmental sustainability: challenges and viable solutions, Environ. Sustain. 1 (4) (2018) 309–340.
- [20] E.A. Baryeh, Effects of palm oil processing parameters on yield, J. Food Eng. 48 (1) (2001) 1–6.
- [21] V. Gibon, W. De Greyt, M. Kellens, Palm oil refining, Eur. J. Lipid Sci. Technol. 109 (4) (2007) 315–335.
- [22] S. Omar, B. Girgis, F. Taha, Carbonaceous materials from seed hulls for bleaching of vegetable oils, Food Res. Int. 36 (1) (2003) 11–17.
- [23] M.R. Ramli, et al., Effects of degumming and bleaching on 3-MCPD esters formation during physical refining, J. Am. Oil Chemists' Soc. 88 (11) (2011) 1839–1844.
- [24] S. Egbuna, Development of kinetic model for adsorption of carotenoids on activated clay in the bleaching of PalmOil, LJRET 3 (1) (2014) 3.
- [25] M.E. Ojewumi, et al., Data on the rheological behavior of cassava starch paste using different models, Data in Brief 19 (2018) 2163–2177.
- [26] M.E. Ojewumi, et al., Statistical optimization and sensitivity analysis of rheological models using cassava starch, Int. J. Civil Eng. Technol. (IJCIET) 10 (1) (2019) 623–639.
- [27] M.E. Ojewumi, et al., In situ bioremediation of crude petroleum oil polluted soil using mathematical experimentation, Int. J. Chem. Eng. (2017) 11. Article ID 5184760.
- [28] M.E. Ojewumi, et al., Optimization of oil from moringa oleifera seed using Soxhlet extraction method, Korean J. Food Health Converg. 5 (5) (2019) 11–25.
- [29] M.E. Ojewumi, Optimization of fermentation conditions for the production of protein composition in parkia biglobosa seeds using response surface methodology, Int. J. Appl. Eng. Res. 12 (22) (2017) 12852–12859.
- [30] M.E. Ojewumi, et al., Extraction of oil from selected plants using Response Surface Methodology [RSM], J. Phys.: Conference Series 1378 (2019), 042019. IOP Publishing.
- [31] F. Akinola, et al., Physico-chemical properties of palm oil from different palm oil local factories in Nigeria, J. Food Agric. Environ. 8 (3&4) (2010) 264–269.
- [32] C.E. Enyoh, et al., Physicochemical parameter of palm oil and soil from Ihube community, Okigwe, Imo State Nigeria, Int. Lett. Nat. Sci. 62 (2017).
- [33] E.E. Chinedu, E.C. Eber, A.C. Emeka, Quality assessment of palm oil from different palm oil local factories in Imo State, Nigeria, World Sci. News 88 (2) (2017) 152–167.
- [34] Aphiar Agnes, E. and R.N. Ikechukwu, Quality Assessment of Physicochemical Properties of Palm Oil from Different Palm Oil Mills in Isoko, Delta State.
- [35] M.E. Ojewumi, Alternative solvent ratios for moringa oleifera seed oil extract, Int. J. Mech. Eng. Res. Technol. 9 (12) (2018) 295–307.
- [36] O.A. Jeje, A. Okoronkwo, O. Ajayi, Effect of bleaching on the physico-chemical properties of two selected vegetable oils using locally sourced materials as adsorbent, Curr. J. Appl. Sci. Technol. (2019) 1–8.
- [37] E. Abdi, M. Gharachorloo, M. Ghavami, Investigation of using egg shell powder for bleaching of soybean oil, LWT 140 (2021) 110859.
- [38] R. Berbesi, Achieving optimal bleaching performance, Oil Mill Gazetteer 112 (2006) 2–6.
- [39] J. Nwabanne, F. Ekwu, Decolourization of palm oil by Nigerian local clay: a study of adsorption isotherms and bleaching kinetics, Int. J. Multidiscipl. Sci. Eng. 4 (1) (2013) 20–27.
- [40] M.S. Hossain, G. Muhammad, Cloud-assisted industrial internet of things (iiot)-enabled framework for health monitoring, Comput. Netw. 101 (2016) 192–202.
- [41] F. Bourgis, et al., Comparative transcriptome and metabolite analysis of oil palm and date palm mesocarp that differ dramatically in carbon partitioning, Proc. Nat. Acad. Sci. 108 (30) (2011) 12527–12532.
- [42] J. Okolo, B. Adejumo, Effect of bleaching on some quality attributes of crude palm oil, J. Eng. 4 (2014) 12.
- [43] M.E. Ojewumi, et al., Optimization of bleaching of crude palm oil using activated groundnut hull, in: International Conference on Engineering for Sustainable World (ICESW 2020). IOP Conf. Series: Materials Science and Engineering, 1107, 2021, 012142.